Conformational Transitions Accompanying Oligomerization of Yeast Alcohol Oxidase, a Peroxisomal Flavoenzyme†

Raina Boteva,‡ Antonie J. W. G. Visser,§ Bruno Filippi,|| Gert Vriend,⊥ Marten Veenhuis,# and Ida J. van der Klei*,#

Institute of Molecular Biology, Bulgarian Academy of Sciences, Sofia 1113, Bulgaria, Department of Biomolecular Sciences, Microspectroscopy Centre, Wageningen Agricultural University, Dreyenlaan 3, 6703 HA Wageningen, Department of Organic Chemistry, University of Padua, 35121 Padua, Italy, EMBL, Meyerhofstrasse 1, 69117 Heidelberg, Germany, and Eukaryotic Microbiology, Groningen Biomolecular Sciences and Biotechnology Institute, Kerklaan 30, 9751 NN Haren, The Netherlands

Received September 21, 1998; Revised Manuscript Received February 8, 1999

ABSTRACT: Alcohol oxidase (AO) is a homo-octameric flavoenzyme which catalyzes methanol oxidation in methylotrophic yeasts. AO protein is synthesized in the cytosol and subsequently sorted to peroxisomes where the active enzyme is formed. To gain further insight in the molecular mechanisms involved in AO activation, we studied spectroscopically native AO from *Hansenula polymorpha* and *Pichia pastoris* and three putative assembly intermediates. Fluorescence studies revealed that both Trp and FAD are suitable intramolecular markers of the conformation and oligomeric state of AO. A direct relationship between dissociation of AO octamers and increase in Trp fluorescence quantum yield and average fluorescence lifetime was found. The time-resolved fluorescence of the FAD cofactor showed a rapid decay component which reflects dynamic quenching due to the presence of aromatic amino acids in the FAD-binding pocket. The analysis of FAD fluorescence lifetime profiles showed a remarkable resemblance of pattern for purified AO and AO present in intact yeast cells. Native AO contains a high content of ordered secondary structure which was reduced upon FAD-removal. Dissociation of octamers into monomers resulted in a conversion of β-sheets into α-helices. Our results are explained in relation to a 3D model of AO, which was built based on the crystallographic data of the homologous enzyme glucose oxidase from *Aspergillus niger*. The implications of our results for the current model of the in vivo AO assembly pathway are discussed.

Methylotrophic yeasts (e.g., *Hansenula polymorpha, Pichia pastoris*) are able to grow on methanol as sole source of carbon and energy. Alcohol oxidase (AO),[1] a homo-octameric enzyme which contains eight, noncovalently bound FAD molecules, catalyzes the first step in methanol metabolism and is located in peroxisomes. AO has been used as a model protein in various studies on peroxisome biogenesis (*1*). Several aspects of AO synthesis and targeting have been elucidated, but relatively little is known on the molecular mechanisms involved in AO translocation and oligomerization.

Like other peroxisomal matrix enzymes, AO is encoded by a nuclear gene and synthesized on free ribosomes in the cytosol. In all organisms studied, the peroxisomal targeting signal of AO resides at the extreme carboxy terminus of the protein and consists of only three amino acids. This targeting sequence, designated PTS1, is recognized in the cytosol by a soluble receptor, Pex5p (*2, 3*). Prior to import, the Pex5p−AO complex is thought to bind to Pex13p and Pex14p, which are both components of a putative docking site on the peroxisomal membrane (*4*−*8*). How the protein is subsequently transported across the peroxisomal membrane and assembled is still largely speculative. Recently, evidences have been presented that specific peroxisomal enzymes such as a PTS1-containing model protein in *Saccharomyces cerevisiae* (*9*) and thiolase in *Yarrowia lipolytica* (*10*) may be imported into the organelle in a folded state. Pulse−chase experiments in *Candida boidinii*, however, suggested that AO is imported as a monomer (*11*). Subsequently, by a genetic approach, additional evidence that translocation of AO precursors into peroxisomes precedes the assembly process was provided (*12*). Hence, active AO octamers are most probably formed in the peroxisomal lumen.

In *H. polymorpha*, FAD binding is apparently a crucial step in AO octamerization. This was indicated by the finding that specific point mutations in the FAD-binding fold strongly affected AO assembly and stability (*13*) and furthermore stressed by the fact that reduced intracellular concentrations of the cofactor FAD prevented AO import and oligomerization (*14*).

Various attempts to reconstitute AO assembly in vitro so far failed. A major reason for this was that denaturation of native AO by urea and KBr led to the irreversible release of FAD from the monomers formed. However, incubation of native AO in 80% glycerol resulted in dissociation of the octamers into FAD-containing monomers, which reassembled

† This work was supported by a short-term fellowship of The Netherlands Organization for Scientific Research (NWO) to R.B.

* Corresponding author. Phone: 31 50 363 2179. Fax: 31 50 363 5205. E-mail: I.J.van.der.Klei@biol.rug.nl.

‡ Bulgarian Academy of Sciences.

§ Wageningen Agricultural University.

|| University of Padua.

⊥ EMBL.

Groningen Biomolecular Sciences and Biotechnology Institute.

[1] Abbreviations: AO, alcohol oxidase; CD, circular dichroism; FAD, flavin adenine dinucleotide; MEM, maximum entropy method; Trp, tryptophan.

10.1021/bi982266c CCC: $18.00
Published on Web 03/31/1999

into the active octamers upon dilution of the glycerol (*15*). Interestingly, reassembly failed when monomers were obtained from octameric AO from which FAD was chemically removed.

Taken together, the current data indicate that binding of FAD to AO protein is not readily achieved in vitro and suggest that in vivo specific proteins (chaperones) may be involved to mediate this process. This was also indicated by the observation that *H. polymorpha* AO failed to bind FAD and to oligomerize when it was synthesized in the heterologous host *S. cerevisiae* (*16*, *17*).

So far, sucrose gradient centrifugation and native gel electrophoresis have been used to monitor the oligomeric state of AO. These methods allow qualitative analyses but have specific drawbacks. For instance, the range in which several parameters (pH, temperature, protein concentration) can be varied is very limited. In addition, these procedures are time-consuming which hampers the detection of instable intermediates and precludes kinetic experiments.

In this paper, we describe the use of different spectroscopic techniques to characterize native AO and different putative assembly intermediates. We show that changes in protein conformation associated with FAD binding and oligomerization can sensitively and quantitatively be monitored by a combination of spectroscopic techniques.

MATERIALS AND METHODS

Proteins. A solution of native *P. pastoris* AO protein in 60% sucrose containing 0.02% NaN_3 was obtained from Provesta Corp. (Bartlesville, OK). AO was purified from *Hansenula polymorpha* as described previously (*18*). The same procedure was used to purify FAD-lacking octameric AO from crude extracts prepared from methanol-grown *H. polymorpha* or *P. pastoris* cells incubated for 2 h at 37 °C in 6 mM KCN (*19*). This treatment resulted in the release of approximately 85−90% of the FAD cofactor from *H. polymorpha* and 70% from *P. pastoris* AO octamers judged from the decrease of the specific FAD absorbance in the visible region. Dissociation of octamers into monomers was achieved by incubation of either the FAD-containing or the FAD-depleted proteins for 2 h at 37 °C in 50 mM potassium phosphate buffer, pH 7.5, containing 80% glycerol (*15*). Protein concentrations were determined from the absorbances at 280 nm using the corresponding molar extinction coefficients of *H. polymorpha* and *P. pastoris* AO calculated on the basis of the aromatic amino acid contents of their monomers (*20*). AO activity was measured at 37 °C for *H. polymorpha* and at 30 °C for *P. pastoris* AO (*21*).

Spectroscopic Measurements. Absorption spectra were recorded using a Beckman spectrophotometer and corrected for light scattering when necessary. AO octamers were measured in 50 mM potassium phosphate buffer, pH 7.5, and monomers in 50 mM potassium phosphate buffer, pH 7.5, containing 80% glycerol. Steady-state fluorescence was measured using a Shimadzu Model RF 5000 spectrofluorometer equipped with a temperature-controlled cuvette holder. Protein concentrations in the range 0.5−1 μM (monomer) were used. Excitation was at 270 nm for Tyr and Trp residues and, selectively, at 295 nm for Trp. Fluorescence of the FAD cofactor was excited at 470 nm. The protein absorbance at the excitation wavelengths was always lower than 0.05 in order to minimize inner filter and self-absorption effects. The relative Trp quantum yield (Q_{Trp}) was calculated by comparing the integrated emission spectra of the proteins excited at 295 nm with that of the standard N-Ac-Trp-NH_2 normalized to the same absorbance at 295 nm. A value of 0.13 was used for the quantum yield of the standard (*22*). The efficiency of Tyr to Trp energy transfer was calculated from the corresponding fluorescence excitation spectra by measuring the dependence of the relative protein quantum yield on the excitation wavelengths (*23*). Quenching of Trp fluorescence was performed using acrylamide as external quencher. The data were analyzed according to the Stern−Volmer equation (*22*). In the case of heterogeneous emission, the modified Stern−Volmer equation was applied. The effect of temperature on conformation was examined by measuring the Trp emission at 340 nm. The samples were kept for 10 min at every temperature prior to measurement to ensure thermal equilibration.

Time-Resolved Fluorescence, Fluorescence Anisotropy Decay. Time-resolved fluorescence and fluorescence anisotropy were measured using the time-correlated single photon counting technique (*24*, *25*). The system was able to accurately resolve fluorescence lifetimes >5 ps (*26*). The excitation and emission wavelengths for Trp decays were 300 and 349 nm, respectively. A red-edge excitation (300 nm) in multi-tryptophan-containing proteins reduces the radiationless energy transfer between tryptophan residues and increases the fundamental anisotropy of tryptophan, hence enhancing the dynamic range of time-resolved fluorescence anisotropy measurements (*27*). For FAD, excitation was at 460 nm, near the absorption maximum of the first electronic transition of the bound flavin (*25*, *26*), and emission at 526 nm. The emission wavelengths were selected with interference filters (Schott, Mainz, Germany). The temperature of the measurements was 22 °C. The fluorescence lifetime distributions were determined from the total fluorescence decay (*28*, *29*) by the maximum entropy method (MEM) using a commercially available program (Maximum Entropy Solutions Ltd., Ely, U.K.). The program also determined the first-order average fluorescence lifetime from the recovered distributed lifetimes with high precision (±1%). Since MEM yields the most probable distribution that is present in the experimental data, one has no control in the number of distributed components that result from such analysis. However, it is sometimes desirable to check whether a simpler decay model applies, for instance when a short correlation time of low amplitude shows up. For this reason, the discrete exponential approach using the global analysis program (Globals Unlimited, Urbana, IL) has been chosen to determine the rotational correlation times (*30*). One cautious remark must be made concerning fluorescence anisotropy decay analysis. Since the fluorescence decay experiment extends only over ca. 30 ns, while the average fluorescence lifetime is only a few nanoseconds, correlation times of about 10 times the average fluorescence lifetime cannot be reliably recovered. In case of very slowly decaying anisotropy, one has to approximate this by fixing the correlation time to a physically realistic value.

Circular Dichroism (CD). CD spectra were determined at 25 °C using a Jasco Model J-715 automatic recording circular dichroism spectrophotometer. Fused quartz cells with a path length of 0.5 cm were used in the visible and near-

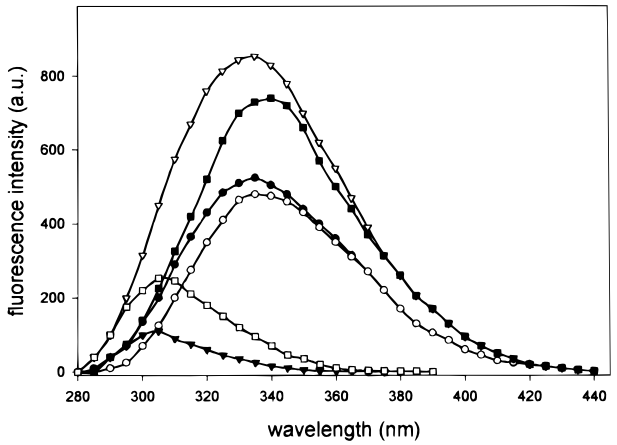

FIGURE 1: Fluorescence emission spectra of 0.8 μM *Pichia pastoris* AO, excited at 270 nm (●, octamer; ▽, monomer) or at 295 nm (○, octamer; ■, monomer). Tyr emission contribution to the fluorescence of octamers (▲) and monomers (□), calculated as the difference between the fluorescence spectra of the two states excited at 270 and 295 nm. The emission spectra (●), (○), and (▲) characterize the octameric state and are obtained in 50 mM potassium phosphate, pH 7.5; (▽), (■), and (□) represent the emission spectra of the monomeric state and are obtained in 50 mM potassium phosphate, pH 7.5, containing 80% glycerol.

UV regions and of 0.1 cm in the far-UV regions. In all CD experiments, the buffer used as blank was separately recorded and subtracted from the sample spectrum. Each spectrum was the average of four scans. Spectra subtraction, normalization, and smoothing were performed using Jasco CD data manipulation J-700 software.

Homology Modeling. The homology modeling of AO based on the glucose oxidase structure was performed using the WHAT IF program (*31*); the WHAT IF homology modeling facility is available as a WWW-based server.

RESULTS

Fluorescence Properties of Octameric and Monomeric Alcohol Oxidase. Based on the deduced amino acid sequences, alcohol oxidase (AO) from the yeast *Hansenula polymorpha* contains 9 Trp and 31 Tyr residues (*32*), whereas the homologous protein from *Pichia pastoris* contains 8 Trp and 33 Tyr residues (*33*). We have analyzed the fluorescence properties of four stable conformational states of the two AO proteins, namely, the native, FAD-containing octamer octamers from which FAD has been chemically removed, and the monomers, derived from either the native or the FAD-lacking octamers. The fluorescence emission spectra of the FAD-containing octamers and monomers of *P. pastoris* (Figure 1) and *H. polymorpha* (spectra not shown) AO are dominated by Trp fluorescence when excited either at 270 nm (where both Tyr and Trp chromophores absorb) or at 295 nm (where predominantly Trp residues absorb); the emission maxima in both cases are at 338 nm for octamers and at 340−342 nm for monomers. The release of FAD did not alter the emission maximum positions (data not shown). Dissociation of *H. polymorpha* and *P. pastoris* native AO octamers into monomers caused a pronounced increase of the relative Trp quantum yields (up to 1.6 times, Table 1).

AO monomers are obtained upon incubation of octameric AO in a solution containing 80% glycerol. Using native gel electrophoresis, Evers et al. (*15*) demonstrated that AO

Table 1: Fluorescence Characteristics, Secondary Structure Content, and Temperatures of Thermal Denaturation of *H. polymorpha* and *P. pastoris* AO[a]

	Q_{Trp}	f_a	K_Q	T_{td} (°C)	α-helix (%)	β-sheet (%)
Hp						
octamer$^+$	0.027	0.40	8.8	49	29	46
monomer$^+$	0.042	0.67	6.1	55	57	–
octamer$^-$	0.028	0.47	5.2	42	22	26
monomer$^-$	0.044	1.00	6.2	60	26	19
Pp						
octamer$^+$	0.030	0.42	8.5	50	32	41
monomer$^+$	0.046	0.80	6.3	51	65	–
octamer$^-$	0.033	0.60	7.4	45	19	28
monomer$^-$	0.057	1.00	6.3	58	24	18

[a] Hp, *H. polymorpha*; Pp, *P. pastoris*; $^+$, FAD-containing AO; $^-$, FAD-lacking AO. Q_{Trp} is the relative Trp quantum yield; K_Q is the Stern−Volmer quenching constant obtained in the presence of acrylamide; f_a is the fraction of accessible fluorescence; T_{td} is the temperature of thermal denaturation calculated from the intercepts of the thermal plots given in Figure 4. Percentages of α-helix and β-sheet secondary ordered structure were calculated from the CD bands in the far-UV region (195−250 nm).

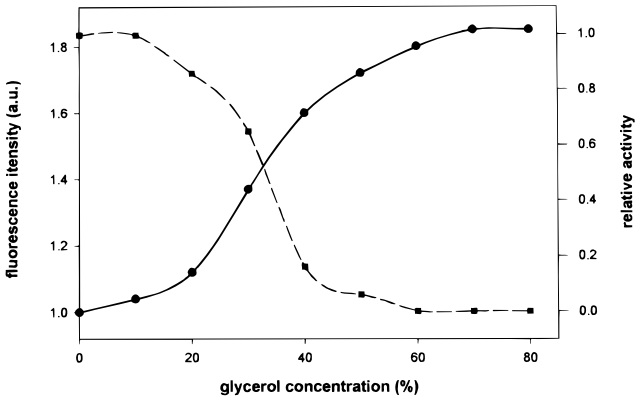

FIGURE 2: Changes in enzyme activity (■) and Trp fluorescence emission (●) upon incubation of native, FAD-containing AO from *P. pastoris* for 2 h, 37 °C, at different concentrations of glycerol. Trp fluorescence was excited at 295 nm and detected at 340 nm and AO activity determined relative to that in untreated controls.

octamers completely dissociate into monomers under these conditions. In addition, this treatment results in a loss of enzyme activity (*15*). We studied the effect of increasing concentrations of glycerol on Trp fluorescence and AO enzyme activity. As shown in Figure 2, increasing concentrations of glycerol resulted in an increase in Trp fluorescence, paralleled by a decrease in AO activity. Both processes are complete at concentrations above 60% glycerol. These data suggest that a direct correlation exists between inactivation of the enzyme and increase in Trp fluorescence, which are a result of dissociation of AO octamers into monomers. Since the fluorescence intensity of free Trp increases significantly in the presence of glycerol (in 80% glycerol the increase is approximately 2-fold), part of the observed increase in Trp fluorescence may be due to the effect of the solvent on exposed Trp residues. However, the sigmoidal character of the curve of fluorescence intensity versus glycerol concentration (Figure 2) and the fact that this dependence exactly corresponds to inactivation of the enzyme indicate that the increase in Trp fluorescence is primarily due to conformational differences between the AO subunits when free or incorporated in octamers.

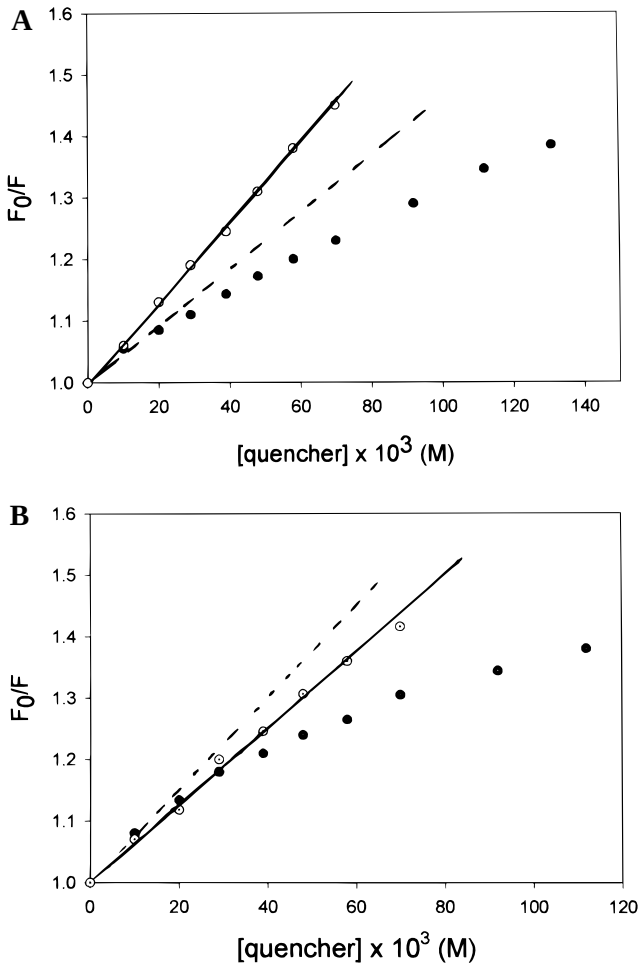

FIGURE 3: Stern−Volmer plots of Trp fluorescence quenching by acrylamide of *H. polymorpha* (A) and *P. pastoris* (B) FAD-depleted alcohol oxidase. Quenching of FAD-depleted octamers (●) was performed in 50 mM phosphate buffer, pH 7.5, and of FAD-depleted monomers (○) in the same buffer containing 80% glycerol. The dashed lines are theoretical and represent the initial slopes, K_Q (Table 1).

The contribution of the Tyr residues to the overall protein fluorescence was calculated to range from 17 to 32% in the different species. Radiationless energy transfer from Tyr to Trp residues could be a reason for the relatively low Tyr emission (*23*). We analyzed that possibility by studying the dependence of protein emission quantum yield on the excitation wavelengths in the 260−300 nm spectral range, but neither in the octameric nor in the monomeric forms of AO could such Tyr−Trp dipole coupling be demonstrated except for FAD-containing octamers of *P. pastoris*, in which minor energy transfer was observed; the efficiency of the process was calculated to amount to approximately 20%, suggesting that 20% of the excitation energy absorbed by Tyr chromophores is transferred via radiationless dipole−dipole interactions to Trp residues.

To localize the emitting Trp, quenching of Trp fluorescence was performed using acrylamide as an external quencher. These experiments revealed a downward curvature of the Stern−Volmer quenching plots for all forms of both proteins except for FAD-depleted monomers (Figure 3A,B), indicating a heterogeneous distribution of the emitting Trp residues (*22*). The fractions of the accessible fluorescence (f_a) and the respective quenching constants (K_Q) associated with these fractions are presented in Table 1. The different values found for f_a support the view that the exposure of the Trp residues to external molecules depends on both the oligomerization state (octameric or monomeric) and FAD binding. In the FAD-containing octamers, approximately 40−42% of the total fluorescence could be quenched by acrylamide, but upon dissociation, this value increased almost 2-fold. Release of the FAD cofactor also resulted in an increase of the accessibility of the Trp chromophores both in monomers and in octamers. Full accessibility of the chromophores toward external solvent molecules ($f_a = 1$, Table 1) was only observed in FAD-depleted monomers. This clearly demonstrates that release of FAD and dissociation of octamers into monomers cause significant conformational rearrangements which decrease the density of the molecule packing and allow easier penetration of the quencher molecules into the interior of the protein. For both native FAD-containing and FAD-lacking octamers, relatively high quenching constants (Table 1) were calculated, typical for accessible Trp residues. The K_Q values for monomers amounted to 6.1−6.3 M^{-1}, which is in the range of the K_Q of free Trp in 80% glycerol which amounts to 6.5 M^{-1}. Due to the high viscosity of glycerol, the latter value is significantly lower compared to free Trp quenching in buffer (*34*). Fluorescence quenching is a dynamic process and requires collision between acrylamide molecules and the excited chromophores. Therefore, enhancement of the medium viscosity hampers quenching of the exposed Trp. This effect is of minor importance for buried residues because for their quenching diffusion of the quencher through the protein and not through the solvent is required (*35*).

Native *H. polymorpha* and *P. pastoris* AO is composed of eight identical subunits, each of which contains one FAD moiety, noncovalently bound. FAD possesses its own fluorescence at 525 nm upon excitation in the visible range (320−520 nm), where protein aromatic residues do not absorb light. It was shown (*36*) that the specific FAD fluorescence in FAD-containing octamers of *P. pastoris* AO is strongly quenched and represents only 4−5% of the emission of free FAD at the same concentration. The specific FAD fluorescence of *H. polymorpha* AO is even weaker than that of *P. pastoris* AO and represents only 1.5% of the free FAD emission. Dissociation of *H. polymorpha* octamers caused a 3.6-fold enhancement in the specific FAD fluorescence intensity; for *P. pastoris* AO, this value was 6.2. In both cases, the increase exceeds the fluorescence increase observed for free FAD upon substitution of phosphate buffer by 80% glycerol (2.3×).

The thermal denaturation plots of the four different forms of *H. polymorpha* and *P. pastoris* AO are shown in Figure 4. Trp fluorescence decreased upon increasing the temperature due to thermal quenching until the temperature of denaturation was reached. Subsequently, an immediate aggregation initiated which caused light scattering and an increase in the signal at 340 nm. The FAD-lacking octamers of the two species seem to be the most unstable states because their aggregation, followed by fast precipitation, was initiated at relatively low temperatures, namely, 42 °C for *H. polymorpha* and 45 °C for *P. pastoris* AO, which are near the optimal growth temperatures of both organisms (Table 1). AO monomers were more resistant toward thermal denaturation as compared to the octamers. FAD-lacking

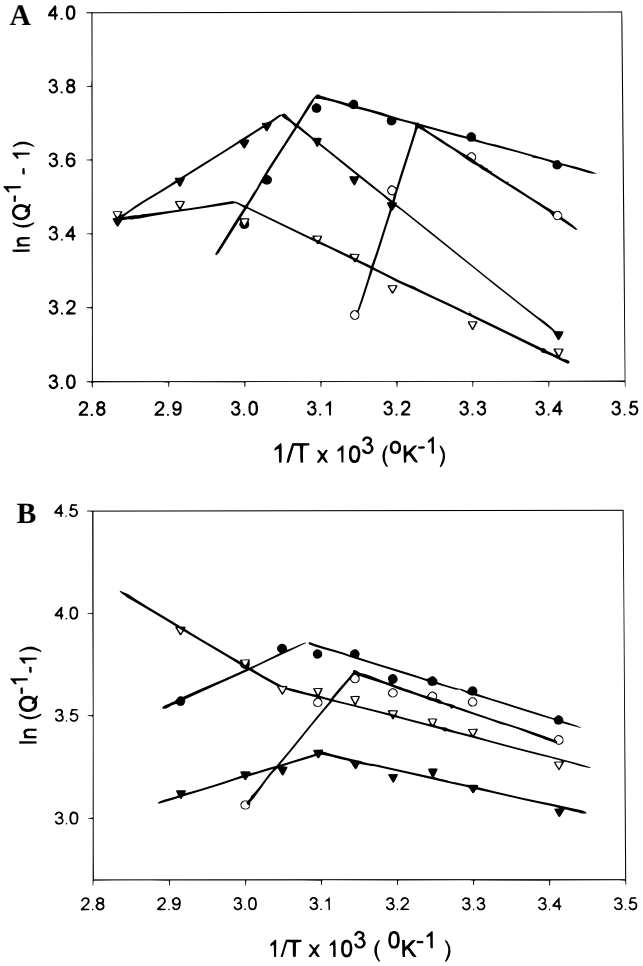

FIGURE 4: Thermal denaturation of *H. polymorpha* (A) and *P. pastoris* AO (B): FAD-containing octamer (●); FAD-containing monomer (▼); FAD-depleted octamer (○) and FAD-depleted monomer (▽), followed at 340 nm. Excitation was at 295 nm. *Q* is determined from the total intensity − Trp emission and light scattering at various temperatures relative to the Trp fluorescence quantum yield at 20 °C, and *T* is the absolute temperature.

monomers denatured at the highest temperatures (58 and 60 °C, Table 1), and up to 80 °C, no light scattering indicative of protein aggregation was observed for the *P. pastoris* FAD-depleted monomers. A likely explanation for the observed higher thermostability of the monomeric forms is the presence of glycerol which has been shown to exert a stabilizing effects on proteins.

Time-Resolved Fluorescence of AO Tryptophan Residues. The fluorescence decay of Trp residues in both FAD-containing and FAD-lacking AO was found to be highly heterogeneous (see Figure 5 for an example of *P. pastoris* FAD-depleted AO). The fluorescence lifetime distribution analysis recovered more than three components, and, therefore, the values of the average lifetimes (τ_{av}) were determined (Figure 5). Dissociation of the octamers into monomers increases the contribution of the longer living components, and, hence, higher values for τ_{av} were obtained, indicating dequenching of Trp chromophores due to conformational rearrangements of the subunits when free and not assembled in octamers. This was also observed for the FAD-containing AO (results collected in Table 2). When freshly prepared FAD-lacking proteins are measured, the fluorescence decay becomes even slower than the one from the monomeric FAD-

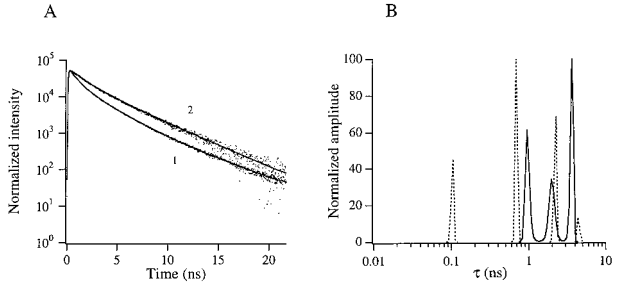

FIGURE 5: Time-resolved fluorescence intensity decay (A) and MEM analysis (B) of tryptophan residues in *P. pastoris* FAD-lacking AO in octameric form (curve 1) and in monomeric form (curve 2) at 295 K. The curves are normalized for clarity. Dotted curves are experimental data, and solid lines are fitted data. The dashed curve (B) corresponds to analysis of curve 1, the solid curve to analysis of curve 2. The fluorescence lifetimes and amplitudes (in parentheses) of octameric AO are 0.10 ns (0.20), 0.69 ns (0.44), 2.19 ns (0.30), and 4.42 ns (0.06), yielding a $\tau_{av} = 1.24$ ns. The fluorescence lifetimes and amplitudes (in parentheses) of monomeric AO are 0.96 ns (0.33), 1.99 ns (0.26), and 3.60 ns (0.41), yielding a $\tau_{av} = 2.37$ ns.

Table 2: Trp Fluorescence Lifetimes and Rotational Correlation Times of FAD-Containing Octameric and Monomeric Forms of *H. polymorpha* and *P. pastoris* Alcohol Oxidases[a]

species	τ_{av} (ns)	β_1 (−)	ϕ_1 (ns)	β_2 (−)	ϕ_2 (ns)
Hp					
octamer	0.99	0.067 (0.058−0.077)	2.5 (1.8−3.9)	0.136 (0.125−0.145)	200
monomer	1.44	0.141 (0.125−0.165)	6.9 (5.2−9.5)	0.112 (0.085−0.130)	2000
Pp					
octamer	1.37	−	−	0.268 (0.264−0.271)	66 (50−82)
monomer	1.79	0.080 (0.055−0.140)	8.6 (4.5−22)	0.207 (0.140−0.230)	2000

[a] Hp, *H. polymorpha*; Pp, *P. pastoris*. τ_{av} is the first-order average fluorescence lifetime as given by the MEM program. The rotational correlation times ϕ_i ($i = 1, 2$) and the corresponding amplitudes β_i are obtained from the global analysis program. The fixed rotational correlation times of 200 and 2000 ns correspond to rotational times of the octameric form and monomeric form in 80% glycerol, respectively. The values in parentheses are obtained from a rigorous error analysis at the 67% confidence level as described in (*30*). For octameric *P. pastoris* alcohol oxidase, a single correlation time was sufficient to approximate the fluorescence anisotropy decay.

containing protein (this is reflected by a longer τ_{av}; $\tau_{av} = 2.37$ ns for FAD-depleted monomer of *P. pastoris* AO and $\tau_{av} = 1.79$ ns for FAD-containing monomer of *P. pastoris* AO). This indicates that Förster-type energy transfer from tryptophan residues to the flavin moiety takes place in the FAD-containing proteins. Energy transfer between the (many) tryptophan residues and FAD in one subunit is very likely as a number of Trp residues are located within the critical transfer distance (ca. 2.0 nm) of a tryptophan−flavin pair (see 3D model in Discussion).

The fluorescence anisotropy decay of the tryptophan residues in *H. polymorpha* octamers is dominated (70% contribution) by a long decay which could not be resolved in time and was set at 200 ns, which is approximately the expected theoretical value for the rotational correlation time of a globular octamer as calculated from the modified Stokes−Einstein relation (*37*, *38*). Another faster component with a barycenter at 2.5 ns contributed about 30% to the

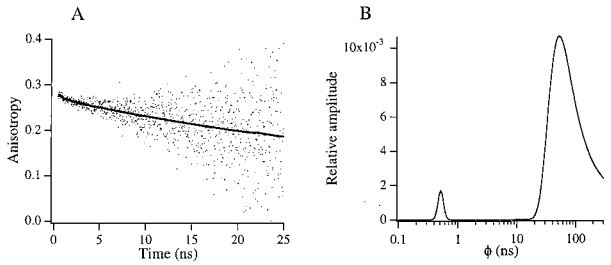

FIGURE 6: Time-resolved fluorescence anisotropy (A) and MEM analysis (B) of tryptophan residues in *P. pastoris* FAD-containing AO in octameric form at 22 °C. The dotted curves (A) are the experimental points, while the solid line represents the fitted anisotropy decay. Two correlation times were found: $\phi_1 = 0.52$ ns (amplitude 0.008) and $\phi_2 = 88$ ns (amplitude 0.260). Fitting with the global analysis program showed that a single correlation time ($\phi = 66$ ns, amplitude 0.268) was sufficient to give an optimal approximation of this decay curve (Table 2).

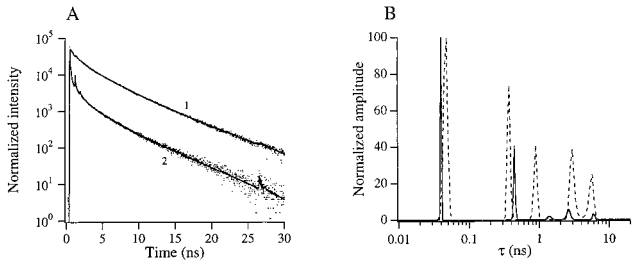

FIGURE 7: Time-resolved fluorescence intensity decay (A) and MEM analysis (B) of FAD in *H. polymorpha* AO in octameric form (curve 1) and in intact cells (curve 2) at 295 K. In cells an ultrarapid decay component is present ($\tau < 10$ ps) which can be clearly seen in the experimental curve 2. This scattering component has been taken into account in the MEM analysis. The normalized lifetime distributions are presented in (B). The fluorescence lifetimes and amplitudes (in parentheses) of isolated AO (dashed curve) are 0.046 ns (0.35), 0.38 ns (0.22), 0.88 ns (0.13), 3.10 ns (0.20), and 5.60 ns (0.10), yielding a $\tau_{av} = 1.2$ ns. The fluorescence lifetimes and amplitudes (in parentheses) of AO in cells (solid curve) are 0.040 ns (0.57), 0.44 ns (0.28), 1.40 ns (0.03), 2.60 ns (0.09), and 5.99 ns (0.03), yielding a $\tau_{av} = 0.61$ ns.

overall anisotropy decay. This reflects either a segmental mobility of chromophores or a remainder of Trp−Trp intramolecular energy transfer. The fluorescence anisotropy decay of the tryptophan residues in *P. pastoris* octamers (Figure 6) is completely dominated (95%) by a slow component of ca. 90 ns (Table 2). The expected theoretical rotational correlation time for a hydrated spherical protein of 75 kDa, which is the molecular mass of one AO monomer, is 30 ns. Therefore, a correlation time in the range 50−100 ns could be attributed to oligomeric forms of the protein. At the short correlation time flanks of the two spectra, components of 0.2 ns (*H. polymorpha*) and 0.5 ns (*P. pastoris*, Figure 6) were also resolved, indicative of rapid reorientational fluctuations of Trp residues within the protein matrix. However, their contributions to the overall fluorescence anisotropy decays are very small and are further decreased upon dissociation of the octamers into monomers. These subnanosecond correlation times are therefore omitted in Table 2.

The changes in the fluorescence anisotropy decay profile registered upon dissociation of AO octamers into monomers could be interpreted only in a qualitative fashion due to the quite different properties of the media in which the octameric and monomeric states are studied. Buffer containing 80% glycerol is characterized by a 60-fold increase of viscosity (*39*), which makes the overall rotational correlation time of the protein 60-fold longer (*40*). Therefore, comparisons of the octamers and monomers with regard to the longer correlation times were not useful. The correlation time distributions of *H. polymorpha* and *P. pastoris* AO monomers are characterized by two main components: one of about 5−7 ns and another unresolved one, set to 2000 ns (roughly 60 times 30 ns, equivalent to an infinitely long anisotropy contribution) (Table 2). The first component reflects internal segmental mobility of Trp residues. The second anisotropy component (2000 ns) can be assigned to overall protein tumbling and was largely predominant, up to 80% in the fluorescence anisotropy decay of *P. pastoris* (Table 2). In both *H. polymorpha* and *P. pastoris* AO monomers, the internal flexibility is relatively higher, because the amplitude β_1 increases in going from octamer to monomer (Table 2).

Time-Resolved Fluorescence of FAD in AO. The time-resolved fluorescence and fluorescence anisotropy of FAD were determined using purified *H. polymorpha* and *P. pastoris* AO protein as well as with a suspension of *H. polymorpha* cells, taking advantage of the fact that AO is the major flavoenzyme in the yeast cells. The fluorescence decay of FAD in AO in intact cells contains an ultrarapid component (see Figure 7) which may arise from scattered light. The fluorescence decays of FAD were strongly heterogeneous, and the lifetime distribution consisted of five peaks with lifetimes in the range from 40 ps to 6 ns (Figure 7). However, the shortest component with a barycenter at 40 ps was predominant and contributed, together with the other subnanosecond lifetimes, 80−95% to the overall decays. Such fast lifetime components strongly suggest effective FAD fluorescence quenching by protein side chains from the FAD-binding pocket.

The two lifetime profiles of FAD obtained with either purified *H. polymorpha* enzyme or intact cells coincide very well. Four out of five lifetime components have approximately the same values, including the dominant 40 ps component. This corroborates the view that fluorescence spectroscopy can be a powerful tool to monitor the dynamics of FAD−protein interactions in vivo.

Fluorescence anisotropy decay analysis of the FAD moiety in the octameric enzyme forms revealed subnanosecond components (results not shown, but data collected in Table 3). Recently, the origin of these short correlation times has been found to be formation of a charge-transfer complex between light-excited flavin and a vicinal aromatic amino acid (*26*). The emission transition moment, located in the plane of the flavin ring, will then change direction upon forming the charge-transfer state. This is a novel fluorescence depolarization mechanism which in principle can occur in a rather rigid flavin environment. It can also be considered as a relaxation mechanism in proteins, since the amino acids surrounding the flavin have to adapt to the charge-transfer state and the reorientation of these amino acids will take place in the subnanosecond time scale.

The longer correlation times (in the 2−8 ns range, see Table 2) of the two enzymes arise most probably from intersubunit energy transfer between the FAD moieties (*25*). In the case of monomeric forms, the longer correlation times

Table 3: FAD Average Fluorescence Lifetimes and Rotational Correlation Times of Octameric and Monomeric Forms of *H. polymorpha* and *P. pastoris* Alcohol Oxidases[a]

species	τ_{av} (ns)	β_1 (−)	ϕ_1 (ns)	β_2(−)	ϕ_2 (ns)	β_3 (−)	ϕ_3 (ns)
Hp							
octamer	1.19	0.130 (0.110−0.149)	0.33 (0.22−0.47)	0.151 (0.136−0.168)	5.8 (4.3−8.4)	0.078 (0.055−0.094)	200
monomer	1.66	−	−	0.291 (0.235−0.330)	5.5 (4.7−6.5)	0.086 (0.055−0.110)	59 (19−ud)
Pp							
octamer	0.96	0.258 (0.224−0.288)	0.21 (0.15−0.26)	0.055 (0.036−0.086)	2.2 (1.1−4.5)	0.035 (0.026−0.041)	200
monomer	2.01	−	−	0.072 (0.034−0.104)	1.1 (0.6−2.5)	0.303 (0.282−0.314)	7.5 (6.8−8.2)

[a] Hp, *H. polymorpha*; Pp, *P. pastoris.* τ_{av} is the first-order average fluorescence lifetime as given by the MEM program. The rotational correlation times ϕ_i (i = 1, 2, 3) and the corresponding amplitudes β_i are obtained from the global analysis program. The fixed rotational correlation time of 200 ns correspond to the rotational time of the octameric form. The values in parentheses are obtained from a rigorous error analysis at the 67% confidence level as described in (*30*). ud means undetermined: any value larger than 19 ns is possible. For the monomer forms, two correlation times are sufficient to approximate the fluorescence anisotropy decay.

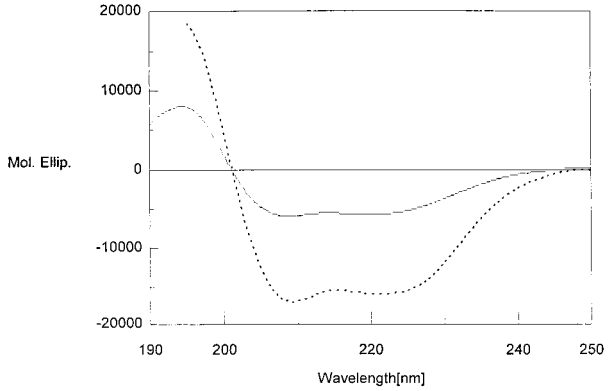

FIGURE 8: Circular dichroism spectra in the far-UV region (195−250 nm) of *H. polymorpha* AO in octameric form, measured in 10 mM potassium phosphate buffer, pH 7.2 (solid line), and in monomeric form (dashed line), measured in the same buffer, containing 80% glycerol.

may also be due to dissociated FAD, which is expected to have a rotational correlation time in the range 4−10 ns for a 80% glycerol solution (Table 3). The contributions of the fixed correlation time of 200 ns in the case of octameric AO and the undetermined correlation time of *H. polymorpha* monomeric AO arise from global protein rotation (Table 3).

CD Characterization of Octameric and Monomeric Forms of AO. The CD spectra of *H. polymorpha* and *P. pastoris* AO in the 195−250 and 250−580 nm spectral ranges are shown in Figures 8 and 9. The percentages of α-helix and *β*-sheet, calculated from the CD bands in the far-UV region, are given in Table 1. The octameric, FAD-containing forms of *H. polymorpha* and *P. pastoris* AO are characterized by 29 and 32% α-helix, and 46 and 41% *β*-sheet, respectively. Both enzymes show complex but very well-resolved CD spectra in the near-UV region (250−320 nm), indicating immobilization of the aromatic side chains in asymmetric environments (Figure 9A,B). The CD spectra of the two enzymes above 320 nm, attributable to the FAD cofactor, show positive Cotton effects. The spectrum of *H. polymorpha* AO octamers (Figure 9A) is characterized by two broad maxima at about 370 and 460 nm, the spectrum of *P. pastoris* AO by one broad band extending up to 580 nm reflecting the FAD−azide complex (Figure 9B).

Dissociation of native AO octamers into monomers in 80% glycerol caused dramatic changes in the ordered secondary

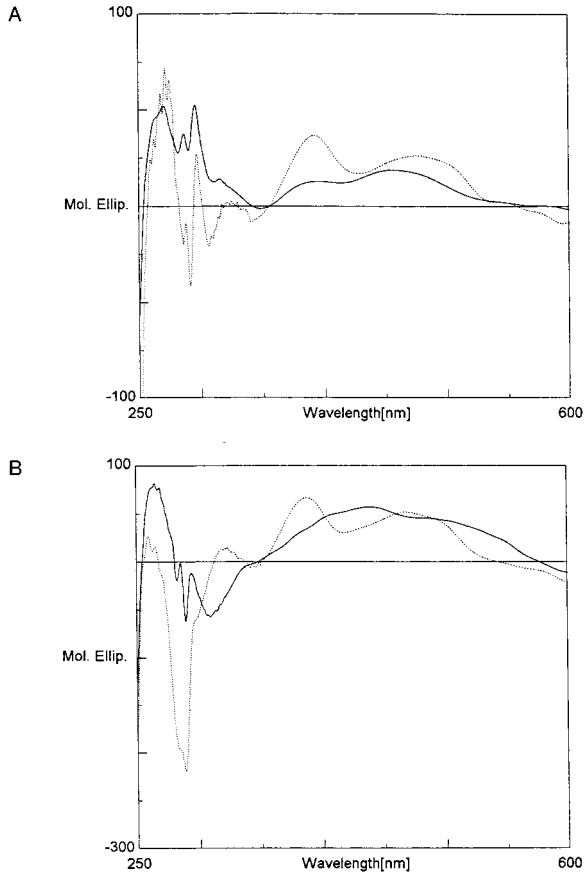

FIGURE 9: Circular dichroism spectra of *H. polymorpha* (A) and *P. pastoris* (B) AO in the near-UV and visible regions (250−600 nm). The solid lines represent the spectra of the octameric forms measured in 10 mM potassium phosphate buffer, pH 7.2, the dashed lines those of the monomeric forms measured in the same buffer, containing 80% glycerol.

structures of the two enzymes. The CD spectra in the far-UV showed the typical features of α-proteins: a deep negative double maximum at 208 and 220 nm and a strong positive band at 195 nm (Table 1, Figure 8). Correspondingly, a significant increase in the percentage of α-helix was observed, and values of 65% in *P. pastoris* and 57% in *H. polymorpha* FAD-containing monomers were calculated. *β*-Sheets seem to completely convert to either α-helices or other aperiodic ordered structures. This redistribution of the

FIGURE 10: Ribbon representation (*50*) of the 3D model of *H. polymorpha* AO. The FAD group and the tryptophan side chains are shown as purple and yellow ball-and-stick models, respectively.

secondary structures in the presence of glycerol clearly indicates drastic rearrangements in the polypeptide folding resulting in disrupture of the quaternary structure organization and dissociation of octamers into monomers. Significant alterations in the near-UV and visible regions concerning both positions and intensity of the CD bands were also observed (Figure 9A,B). The aromatic side chains remain immobilized in rather rigid, asymmetric environments as suggested by their well resolved CD spectra, but the sign and the magnitude of the bands change, indicating alterations in their structural and electronic environment. The CD spectra in the 320−580 nm region, attributable to FAD, consist of two positive broad bands with maxima at aproximately 370 and 460 nm. The relative differences in rotational strengths of these absorption transitions as compared to native octamers indicate subtle changes in the flavin microenvironment. They further indicate that FAD is clearly bound in both octameric and monomeric states since dissociated FAD would display hardly any Cotton effect (*40*).

Significant reduction of the ordered secondary structure contents is observed upon removal of the FAD cofactor (Table 1). Drastic changes in the aromatic region were observed as well. The fine structure characteristic of FAD-containing states is replaced by a broad, very low intensity minimum at 280 nm which completely disappears upon dissociation of the FAD-lacking octamers into monomers. The last state is characterized by the highest percentage of unordered structure of approximately 55% (*H. polymorpha*) and 58% (*P. pastoris*). However, a slight increase of the α-helix content in the FAD-depleted monomers as compared to the FAD-depleted octamers was observed, reflecting the effect of glycerol on secondary structure redistribution.

Homology Modeling. Because a 3D structure of AO is not available yet, a model was built based on the known structure of a homologous protein. AO shows little sequence homology with any known PDB file. A BLAST search (*41*) revealed a marginal homology with *Aspergillus niger* glucose oxidase [~25% sequence identity; PDB file 1gal; (*42*)]. Threading programs such as TOPITS (*43*) revealed no other structures that would be a better candidate template file. At this level of sequence identity, homology modeling is generally considered difficult. Consequently, the sequence alignment had to be optimized by hand. This was done in an iterative manner, using model characteristics such as buried charged residues, too long gap distances, etc. as guidelines. The details of the sequence alignment procedure are available (http://swift.embl-heidelberg.de/service/gal/). A ribbon representation of the AO model is given in Figure 10.

DISCUSSION

We have studied four different conformational states of the flavoenzyme alcohol oxidase (AO) from the methylotrophic yeasts *Hansenula polymorpha* and *Pichia pastoris*, including potential assembly intermediates. Apart from the native enzyme (FAD-containing octamers), we have characterized FAD-lacking octamers as well as the corresponding monomers.

Because no 3D structure is available yet for AO, we have built a model based on the known structure of the enzyme glucose oxidase, which has approximately 25% sequence identity with AO. This model may reflect the conformation of AO subunits present in the native enzyme. Because glucose oxidase is a dimer, the available data did not allow design of a 3D model for the AO octamer. At about 25% sequence identity between template and model, modeling is clearly possible (*44*), but generally considered difficult, and errors are expected to be present in several surface loops (*45*). However, one can still be reasonably sure that the proteins have a similar fold, and in case of enzymes one can be sure of a higly similar active site. The fine details of the AO modeling process are available from the WWW (http://swift.embl-heidelberg.de/service/gal), but in summary it can be concluded that although the fine details of the model

are surely going to be in error, the overall features such as, for example, the asymmetric clustering of Trp residues will most likely be correct. According to the model, most Trp residues seem to be shielded by the protein matrix except three which may be fully or partially exposed to the solvent. This location heterogeneity is reflected by the observed Trp fluorescence distinguishing at least two different classes of chromophores: accessible to the solvent or buried in the hydrophobic interior of protein where it is inaccessible for external quencher. The fractions of the exposed chromophores were strongly dependent on the oligomerization state and FAD binding and increased upon dissociation of the octamers into monomers and release of the cofactor (Table 1), reaching 100% in FAD-lacking monomers of both AO proteins studied.

Characteristics of the Native Protein (FAD-Containing Octamer). Native, FAD-containing AO octamers are characterized by the highest content of ordered secondary structure: 75% (*H. polymorpha*) and 73% (*P. pastoris*) α-helices and β-strands, judged from CD analysis. Aromatic residues are immobilized in an asymmetric environment as suggested by their complex but well-resolved CD spectrum in the near-UV. Analysis of fluorescence anisotropy decay may point to some intramolecular Trp−Trp homoenergy transfer, often observed in multi-tryptophan proteins (*27*), which also may occur in the case of AO since clusters of Trp residues could be identified in the model (Figure 10). The FAD moiety is optically active and shows rather intensive positive Cotton bands in the visible region, indicative of immobilization of this cofactor within the protein matrix. The highly heterogeneous FAD fluorescence and anisotropy decay pattern and the predominance of short-living components indicate strong quenching of the flavin moiety by protein side chains in the FAD-binding pocket. This conclusion is supported by steady-state fluorescence measurements which showed that the emission of the FAD cofactor is approximately 2 orders of magnitude lower as compared to that of free FAD. Inspection of the model identifies at least two Tyr and two Cys residues in the FAD-binding pocket which could be potential quenchers of FAD fluorescence. Phe is less likely to quench, as recently shown (*26*). Ultrashort fluorescence lifetimes have been observed in other flavoproteins as well (*25*, *26*). Recently, a photochemical explanation for picosecond lifetime components as observed in flavoproteins with largely quenched flavin fluorescence such as AO and glutathione reductase was presented (*26*). It is based on an excited-state reaction in which light-excited flavin extracts an electron from a vicinal aromatic amino acid (Tyr or Trp). Such a charge-transfer state leads to a very short fluorescence lifetime, and when the flavin reaches the ground state, the original situation is restored. Evidence for this mechanism came from site-directed mutagenesis experiments of glutathione reductase which showed that, after substitution of the Tyr close to the flavin by another amino acid, the shortest lifetime component largely disappeared. The longer correlation times observed in the octameric proteins indicate intersubunit radiationless homoenergy transfer between FAD moieties from different subunits. These interactions are probably assisted by intermolecular β-sheets which stabilize the quaternary protein structure (*42*) and are disrupted in the presence of high glycerol concentrations, causing dissociation of octamers into monomers as suggested by the CD data.

FAD-Containing Monomers. Dissociation of FAD-containing octamers into monomers resulted in drastic perturbations in the ordered secondary structure content reflected by the increase in percentage α-helices at the expense of β-sheets, which were in part converted to α-helices and for the remaining part into other aperiodic ordered structures. The profiles of the CD spectra in the near-UV and visible regions also changed, indicating differences between monomeric and octameric states with respect to the microenvironments of both the aromatic residues and the FAD cofactor. However, the two chromophoric species remained immobilized within the protein matrix as indicated by their high optical activities in the near-UV and visible regions.

Monomers possess a higher internal flexibility and permeability, allowing easier penetration of small external molecules in the protein globule. They are also characterized by higher average fluorescence lifetime and Trp emission quantum yield than the octamers. This observation indicates some dequenching of Trp chromophores as a result of conformational rearrangements of the subunits and disruption of the quaternary structure. Fluorescence anisotropy decay patterns characteristic of free FAD in 80% glycerol were also identified, suggesting that a portion of FAD molecules dissociates. These findings may explain previous results of other authors (*15*), who were unable to fully reconstitute AO activity by reassociation of glycerol-treated AO.

FAD-Depleted Octamers. Release of FAD from AO octamers caused significant conformational destabilization as deduced from the thermal denaturation profiles of the two FAD-lacking enzymes. Temperature-induced denaturation and aggregation were found to initiate at a relatively low temperature, close to the optimal growth temperature of *H. polymorpha* and *P. pastoris*. The CD spectra revealed that the FAD-depleted octamers contained significantly less ordered secondary structure as compared to FAD-containing forms. This finding correlates with the completely changed CD profile in the near-UV region where one broad, very weak negative band around 280 nm substituted the complex fine structure in the CD spectra of the FAD-containing states. These results clearly indicate significant changes in the microenvironment and increase in the mobility of the aromatic side chains after FAD removal. The positions of the Trp residues in the 3D model do not suggest that they are part of the FAD-binding site. Three of them might be at a shorter distance than 10 Å to the FAD moiety and are suitable for efficient Trp−FAD dipole−dipole coupling, but the orientation of their side chains seems to be unfavorable for this type of interaction. Nevertheless, the FAD-depleted protein definitely exhibits a slower fluorescence decay than the FAD-containing species which is indicative of radiationless energy transfer via dipole−dipole coupling from Trp residues to the flavin cofactor. These tryptophans will have a shorter fluorescence decay time, since energy transfer is an extra pathway to depopulate the excited state and will reduce their lifetime. Hence, the average fluorescence lifetime will be shorter in the holoenzyme than in the apoenzyme. The occurrence of conformational changes will not invoke all Trp residues: some of the tryptophans will change their microenvironment, but most Trp residues will retain their relative positions with respect to the flavin.

FAD-Depleted Monomers. FAD-depleted monomers are characterized by the highest accessibility of the Trp residues indicative of a quite loosely packed conformation. Many of the spectral characteristics, such as lowest percentage of ordered secondary structure, the absence of any signal in the aromatic CD region, flexible and relaxed tertiary conformation, and high resistance toward thermal denaturation, qualify the FAD-depleted monomer as an earlier stage in the AO folding/assembly pathway.

The in Vivo AO Assembly Pathway. In vivo FAD-lacking AO monomers are synthesized in the cytosol which are considered to be the first intermediates in the AO assembly pathway. Our current studies revealed that this conformation is very flexible and only loosely folded. Most probably FAD binds to this state in vivo, followed by oligomerization of the subunits. FAD-lacking octamers do not seem probable intermediates in AO assembly judged from their conformational fragility at relatively low temperatures near the optimal growth temperatures of the organisms. Our current data show significant conformational differences between the FAD-containing and FAD-lacking octameric and monomeric forms. Hence, it is likely that molecular chaperones are necessary to allow FAD binding in vivo.

Incubation in Glycerol Strongly Affects AO Protein Conformation. Incubation of octameric AO in 80% glycerol severely affects the protein conformation and induces structural rearrangements leading to stabilization of the α-helices. Recently, it was found that peptides can form different secondary structures, either α-helices or β-strands, with a marginal difference between the free energies of stabilization (*46*, *47*). Glycerol was shown to increase the protein internal hydrophobicity and to favor structural conversions leading to better stabilization of α-helices which prefer a hydrophobic environment (*48*−*50*). Recent studies have shown that the molecular bases for protein polymerization which causes fatal neurodegenerative illness of animals and humans ("prion diseases") are conformational transitions of α-helices into β-strands. It was also found that glycerol, as a chemical chaperone, interferes successfully with this process by stabilizing the α-helical structures and preventing formation of intermolecular β-sheets. Possibly, the effects of glycerol on the oligomeric state of AO are also due to stabilization of α-helices at the expense of β-structures, which might be important for intersubunit contacts.

ACKNOWLEDGMENT

Arie van Hoek is thanked for his assistance in the time-resolved fluorescence experiments.

REFERENCES

1. Van der Klei, I. J., Harder, W., and Veenhuis, M. (1991) *Yeast 7*, 195−209.
2. McCollum, D., Monosov, E., and Subramani, S. (1993) *J. Cell Biol. 121*, 761−774.
3. Van der Klei, I. J., Hilbrands, R. E., Swaving, G. J., Waterham, H. R., Vrieling, E. G., Titorenko, V. I., Cregg, J. M., Harder, W., and Veenhuis, M. (1995) *J. Biol. Chem. 270*, 17229−17236.
4. Erdmann, R., and Blobel, G. (1996) *J. Cell Biol. 135*, 111−121.
5. Elgersma, Y., Kwast, L., Klein, A., Voorn-Brouwer, T., Van den Berg, M., Metzig, B., America, T., Tabak, H. F., and Distel, B. (1996) *J. Cell Biol. 135*, 97−109.
6. Gould, S. J., Kalish, J. E., Morell, J. C., Bjorkman, J., Urquhart, A. J., and Crane, D. I. (1996) *J. Cell Biol. 135*, 85−95.
7. Komori, M., Rasmussen, S. W., Kiel, J. A. K. W., Baerends, R. J. S., Cregg, J. M., Van der Klei, I. J., and Veenhuis, M. (1997) *EMBO J. 16*, 44−53.
8. Albertini, M., Rehling, P., Erdmann, R., Girzalsky, W., Kiel, J. A. K. W., Veenhuis, M., and Kunau, W. H. (1997) *Cell 89*, 83−92.
9. McNew, J. A., and Goodman, J. M. (1994) *J. Cell Biol. 127*, 1245−1257.
10. Glover, J. R., Andrews, D. W., and Rachubinski, R. A. (1994) *Proc. Natl. Acad. Sci. U.S.A.* 91, 10541−10545.
11. Goodman, J. M., Scott, C. W., Donahue, P. N., and Atherton, J. P. (1984) *J. Biol. Chem. 259*, 8485−8493.
12. Waterham, H. R., Russell, K. A., De Vries, Y., and Cregg, J. M. (1997) *J. Cell Biol. 139*, 1419−1431.
13. De Hoop, M. J., Aesgeirsdottir, S., Blaauw, M., Veenhuis, M., Cregg, J. M., and Ab, G. (1990) *Protein Eng. 4*, 821−829.
14. Evers, M. E., Titorenko, V. I., van der Klei, I. J., Harder, W., and Veenhuis, M. (1994) *Mol. Biol. Cell 5*, 829−837.
15. Evers, M., Harder, W., and Veenhuis, M. (1995) *FEBS Lett. 368*, 293−296.
16. Distel, B., Veenhuis, M., and Tabak, H. F. (1987) *EMBO J. 6*, 3111−3116.
17. Van der Klei, I. J., Veenhuis, M., Van der Leij, I., and Harder, W. (1989) *FEMS Lett. 57*, 133−138.
18. Van der Klei, I. J., Bystrykh, L. V., and Harder, W. (1990) *Methods Enzymol. 188*, 420−427.
19. Van der Klei, I. J., Veenhuis, M., Nicolay, K., and Harder, W. (1989) *Arch. Microbiol. 151*, 26−33.
20. Beaven, G. H., and Holiday, E. R. (1952) *Adv. Protein Chem. 7*, 319−325.
21. Verduyn, C., Van Dijken, J. P., and Scheffers, W. A. (1984) *J. Microbiol. Methods 2*, 15−25.
22. Lehrer, S. S. (1971) *Biochemistry 10*, 3254−3263.
23. Eisinger, G. (1969) *Biochemistry 8*, 3902−3907.
24. Pap, E. H. W., Bastiaens, P. I. H., Borst, J. W., Van den Berg, P. A. W., Van Hoek, A., Snoek, G. T., Wirtz, K. W. A., and Visser, A. J. W. G. (1993) *Biochemistry 32*, 13310−13317.
25. Bastiaens, P. I. H., Van Hoek, A., Wolkers, W. F., Brochon, J. C., and Visser, A. J. W. G. (1992) *Biochemistry 31*, 7050−7060.
26. Van den Berg, P. A. W., Van Hoek, A., Walentas, C. D., Perham, R. N., and Visser, A. J. W. G. (1998) *Biophys. J. 74*, 2046−2058.
27. Khmelnitsky, Y. L., Van Hoek, A., Veeger, C., and Visser, A. J. W. G. (1993) *Eur. J. Biochem. 212*, 63−67.
28. Livesey, A. K., and Brochon, J. C. (1987) *Biophys. J. 52*, 693−706.
29. Brochon, J. C. (1994) *Methods Enzymol. 240*, 262−311.
30. Beechem, J. M., Gratton, E., Ameloot, M., Knutson, J. R., and Brand, L. (1991) in *Topics in Fluorescence Spectroscopy* (Lakowicz, J. R., Ed.) Vol. 2, pp 241−305, Plenum, New York.
31. Rodriguez, R., Chinea, G., Lopez, N., Pons, T., and Vriend, G. (1998) *Bioinformatics 14*, 523−528.
32. Ledeboer, A. M., Edens, L., Maat, J., Visser, C., Bos, J. W., and Verrips, C. T. (1985) *Nucleic Acids Res. 13*, 3063−3082.
33. Ellis, S. B., Brust, P. F., Koutz, A. T., Waters, M. M., Harphold, and Gingeras, T. R. (1985) *Mol. Cell Biol. 5*, 1111−1121.
34. Ricchelli, F., Jori, J., Shopova, M., Boteva, R., and Genov, N. (1981) *Int. J. Pept. Protein Res. 17*, 330−337.
35. Eftink, M. R., and Ghiron, C. A. (1976) *Biochemistry 15*, 672−680.
36. Couderc, R., and Baratti, J. (1980) *Agric. Biol. Chem. 44*, 2279−2289.
37. Visser, A. J. W. G., and Lee, J. (1980) *Biochemistry 19*, 4366−4372.
38. Vos, K., Van Hoek, A., and Visser, A. J. W. G. (1987) *Eur. J. Biochem. 165*, 55−63.
39. Handbook of Chemistry and Physics, 56th ed. (1975−1976), p D-231, CRC Press, Cleveland.

40. Visser, A. J. W. G., Van Berkel, W. J. H., and De Kok, A. (1995) *Biochim. Biophys. Acta 1229,* 381−385.
41. Altschul, S. F., Gish, W., Miller, W., Myers, E. S., and Lipman, D. J. (1990) *J. Mol. Biol. 215,* 403−410.
42. Hecht, H. J., Kalisc, H. M., Hendle, J., Schmid, R. D., and Schomburg, D. (1993) *J. Mol. Biol. 229,* 153−172.
43. Rost, B. (1995) in TOPITS: Threading One-dimensional Predictions Into Three-dimensional Structures (Rawlings, C., Clark, D., Altman, R., Hunter, L., Lengauer, T., and Wodak, S., Eds.) pp 314−321, AAAI Press, Cambridge, U.K.
44. Chothia, C., and Lesk, A. M. (1986) *EMBO J. 5,* 823−836.
45. Sander, C., and Schneider, R. (1991) *Proteins: Struct., Funct., Genet. 9,* 56−68.
46. Perutz, M. F. (1997) *Nature 385,* 773−775.
47. Minor, D. L., and Kim, P. S. (1996) *Nature 380,* 730−734.
48. Zhang, H., Kaneko, K., Nguyen, J., Livshits, T. L., Baldwin, M. A., Cohen, F. E., James, T. L., and Prusiner, S. B. (1995) *J. Mol. Biol. 250,* 514−526.
49. Tatzelt, J., Prusiner, S. B., and Welch, W. J. (1996) *EMBO J. 15,* 6363−6373.
50. Booth, D. R., Sunde, M., Bellotti, V., Robinson, C. V., Hutohinson, W. L., Fraser, P. E., Hawkins, P. N., Dobson, C. M., Radford, S. E., Blake, C. C. F., and Pejys, M. B. (1997) *Nature 385,* 787−793.
51. Carson, M. (1987) *J. Mol. Graph. 5,* 103−106.

BI982266C